Journal of Operation and Automation in Power Engineering

Vol. 5, No. 2, Dec. 2017, Pages: 227-239

http://joape.uma.ac.ir

Optimal Operation Management of Grid-connected Microgrid Using Multi-Objective Group Search Optimization Algorithm

H. Shayeghi[*], *E. Shahryari*

Department of Technical Engineering, University of Mohaghegh Ardabili, Ardabil, Iran.

Abstract- *Utilizing distributed generations (DGs) near load points has introduced the concept of microgrid. However, stochastic nature of wind and solar power generation as well as electricity load makes it necessary to utilize an energy management system (EMS) to manage hourly power of microgrid and optimally supply the demand. As a result, this paper utilizes demand response program (DRP) and battery to tackle this difficulty. To do so, an incentive-based DRP has been utilized and the effects of applying DRP on microgrid EMS problem have been studied. The objective functions of microgrid EMS problem include the total cost and emission. These metrics are combined in a multi-objective formulation and solved by the proposed multi-objective group search optimization (MOGSO) algorithm. After obtaining Pareto fronts, the best compromise solution is determined by using fuzzy decision making (FDM) technique. Studies have been employed on a test microgrid composed of a wind turbine, photovoltaic, fuel cell, micro turbine and battery while it is connected to the upper-grid. Simulation results approve the efficiency of the proposed method in hourly operation management of microgrid components.*

Keywords: Microgrid, Demand response program, MOGSO, Fuzzy decision making, Wind turbine.

NOMENCLATURE

Abbreviations

DG	distributed generation
DRP	demand response program
EMS	energy management system
FDM	fuzzy decision making
FC	fuel cell
GSO	group search optimization
IBP	incentive-based program
MOGSO	multi-objective group search optimization
MT	micro turbine
PBP	price-based program
PV	Photovoltaic
SOC	state of charge
UG	upper-grid
WT	wind turbine

Parameters

$A(i)$	incentive payment in ith hour
$d_0(i)$	initial load in i^{th} hour
$E(i,i)$	self-elasticity
$E(i,j)$	cross elasticity
N_G	number of DGs
N_{SS}	number of storage systems
$pen(i)$	penalty in ith hour
$SG_i(t)$	start-up and shut-down costs of DGs
$S_{si}(t)$	start-up and shut-down costs of storage system
T	index of hours
$\eta_{chargej}$	storage's charge efficiency
$\eta_{dischargej}$	storage's discharge efficiency
$\rho_0\ (j)$	initial price in j^{th} hour

Variables

$B(d(i))$	revenue of customer in ith hour
$C_{Gi}(t)$	hourly price for DGs
$C_{si}(t)$	hourly price of storage system power
$C_{EX}(t)$	hourly exchanged power for UG
$d(i)$	customer demand in i^{th} hour
$E(t)$	emission in t^{th} hour
$\rho(i)$	spot electricity price in i^{th} hour
$P_{Gi}(t)$	hourly power of DGs
$P_{si}(t)$	hourly storage system power
$P_{EX}(t)$	hourly exchanged power with UG
S	total profit of consumer
u_{GNG}	on/off state of DGs
u_{SNSS}	on/off state of storage units
$X(t)$	vector of variables

Received: 22 May 2017
Revised: 4 July 2017
Accepted: 8 Agu. 2017
∗Corresponding author:
E-mail: *hshayeghi@gmail.com (H. Shayeghi)*
Digital object identifier: 10.22098/joape.2017.3659.1290

$W_{Sj}(t)$ SOC of j^{th} storage unit

1. Introduction

During the recent years, growing utilization of clean energy sources along with decreasing consideration of fossil fuels have motivated researchers to modify the generation and transmission form of the electricity power [1]. As a result, distributed generations are emerged by technical improvement of the renewable energy sources [2]. Hence, the electricity consumption is provided near load points and at lower voltage level by non-conventional DGs (such as FCs) along with renewable ones (such as WTs and PV systems) [3]. This strategy has introduced microgrid as a new concept which is constructed by aggregation of loads, storage systems, renewable and non-conventional DGs while generates and distributes electricity within a specified area near loads. Microgrids can be operated in grid-connected or stand-alone mode. During the first one, the system is able to exchange power with UG. However, during the latter one which is also named islanded mode, microgrid is completely separated from the utility [4]. Since generated power of renewable DGs is dependent to weather condition and as a result of loads variable nature, microgrids require an EMS to balance generation-consumption [5]. An EMS tries to take the most advantage of DGs and it fails to supply the load if the generation is less than consumption. In such a situation, utilizing backup systems like battery and DRP are suggested to reduce the power mismatch [6]. The battery saves power during cheap and off-peak hours to discharge it in peak hours [7]. Diverse studies have been paid attention to utilization of battery in microgrid EMS [8]. Authors of [9] have employed battery to overcome uncertainties of wind power which are generated as a result of prediction error and solved EMS problem of microgrid using multi-objective optimization. However, in [10] microgrid EMS is solved in presence of battery using distributed intelligence and multi-agent systems. In Ref. [11], battery is considered as a reserve energy source and EMS is solved using point estimated method. Another solution to tackle this problem and provide generation-consumption balance is to decrease customer's consumption during the system's shortage hours. This reserve which is provided by demand side and is able to participate in power market is called DRP [12]. As a result, various studies have been done to manage DRP in microgrids EMS. Totally, DRPs are classified into PBPs and IBPs which are formulated as price elasticity model to participate in power market [13]. However, the elasticity model is not able to model discrete features of load and obtaining the exact price-elastic curve of demand is so difficult [14]. The utilized DRP in [15], is a price-offer package which formulates load curtailment of residential, commercial and industrial consumers to manage EMS of a microgrid. The same DRP is utilized by authors of [16] to manage generation uncertainty of microgrid DGs by using multi-objective optimization. Considering the positive effects of DRPs, load reduction has a negative effect on psychology of consumers especially the industrial ones. Authors of Ref. [17] have considered these bad psychological effects and replaced the load reduction with load shifting in microgrid EMS. An improved DRP model is presented in [18] which has maximized the microgrid benefit by considering interruptible and uninterruptible loads, simultaneously.

Combining both of aforementioned solutions, battery and DRP, makes microgrid more reliable and has attracted lots of attention in the literature [19]. Combination of load reduction and battery in microgrid are studied in [20] while considering security risks. However, their simultaneous implementation is solved by authors of [21] as a multi-objective problem. Furthermore, microgrid EMS in a system containing PV, WT, DRP and battery is solved by zhao et al. [22] using multi-agent system.

The abovementioned papers have considered load reduction as a reserve energy source and have neglected load shifting. As a result, the effects of self and cross elasticity concepts are not considered. In addition, they have solved multi-objective microgrid EMS problem using common multi-objective optimization algorithms. However, in this paper, a multi-objective scheduling model for microgrid EMS problem solution is presented to minimize the total cost and emission of microgrid. The formulated EMS problem is solved using the proposed MOGSO algorithm while the multi-objective utilization of GSO algorithm was not implemented before. The understudying microgrid is composed of a WT, PV, FC and MT while it is connected to the UG. As a result of uncertainties related to WT, PV and load and to cover them, a battery and an incentive-based DRP are considered in the operation management of microgrid. Utilization of DRP has added load shifting as a reserve energy source and considered the effects of self and cross elasticity concepts which were not taken into account at the abovementioned papers. To reach this goal, load curve is divided into three intervals which has different

elasticity with respect to the price changes.

Totally, the main contributions of this paper are summarized as bellow:

- Self and cross elasticity concepts are considered in solving microgrid EMS problem.
- Load shifting is considered as a reserve energy source.
- The proposed MOGSO algorithm is utilized to solve the multi-objective problem of microgrid EMS.

The rest of the paper is organized as follows: The mathematical formulation of objective functions along with constraints are presented in Section 2. In Section 3, a brief introduction of multi-objective group search optimization algorithm is presented. The numerical results and conclusions are presented in Section 4 and 5, respectively.

2. Problem formulation

In this section, mathematical formulation of microgrid operation management is presented. Minimization of two objective functions including operation cost in €ct (Euro cent) and pollutant emission in kg are considered in this paper. Furthermore, DRP and storage system are taken into account as two flexible energy sources in order to cover problem uncertainties.

2.1. DRP

An economic incentive-based DRP is considered here to formulate participation of consumers in the demand response [13]. In this regard, self-elasticity is defined as the sensitivity of load with respect to price of the same time horizon as bellow:

$$E = \frac{\rho_0}{d_0}.\frac{\partial d}{\partial \rho} \tag{1}$$

However, cross-elasticity can be obtained by sensitivity of load at i^{th} hour to price of j^{th} hour as following:

$$E(i,j) = \frac{\rho_0(j)}{d_0(i)}.\frac{\partial d(i)}{\partial \rho(j)} \tag{2}$$

Changes in price of electricity during various time horizons may result in one of the following cases:

- Some of loads such as lightning cannot be transferred to another time horizon. So, they have just self-elasticity which is always negative.
- A number of loads can be transferred from peak hours to off-peak ones. As a result, self-elasticity (*E(i,i)*) and cross-elasticity (*E(i,j)*) can be defined for them as bellow:

$$\begin{cases} E(i,i) \le 0 \ \ if \ \ \ i = j \\ E(i,j) \ge 0 \ if \ \ \ i \ne j \end{cases} \tag{3}$$

2.1.1. DRP with self-elasticity

A consumer modifies his load from *d0(i)* to *d(i)* according to incentive and penalty payments.

$$\Delta d(i) = d(i) - d_0(i) \tag{4}$$

Considering *A(i)* in $ as the incentive payment for per kWh load reduction of consumer at i^{th} hour, total incentive of the consumer for participating in DRP is:

$$P(\Delta d(i)) = A(i)[d(i) - d_0(i)] \tag{5}$$

If the engaged consumer does not fulfill his commitments, he will be faced with a penalty. Assuming *IC(i)* and *pen(i)* as the amount of commitment at i^{th} hour and the value of penalty for each hour, respectively, total penalty value is as follow:

$$PEN(\Delta d(i)) = pen(i)\{IC(i) - [d(i) - d_0(i)]\} \tag{6}$$

Furthermore, by considering *B(d(i))* as the revenue of consumer at i^{th} hour for utilizing *d(i)* kWh of electricity power, total profit of consumer (S) at i^{th} hour is:

$$S = B(d(i)) - d(i).\rho(i) + P(\Delta d(i)) - PEN(\Delta d(i)) \tag{7}$$

According to optimization rules, the profit is maximum when $\frac{\partial S}{\partial d(i)}$ equals to zero. So:

$$\frac{\partial S}{\partial d(i)} = \frac{\partial B(d(i))}{\partial d(i)} - \rho(i) + \frac{\partial P}{\partial d(i)} - \frac{\partial PEN}{\partial d(i)} = 0 \tag{8}$$

$$\frac{\partial B(d(i))}{\partial d(i)} = \rho(i) + A(i) + pen(i) \tag{9}$$

Assuming the profit function as a quadratic function as bellow:

$$B(d(i)) = B_0(i) + \rho_0(i)[d(i) - d_0(i)]\left\{1 + \frac{d(i) - d_0(i)}{2E(i).d_0(i)}\right\} \tag{10}$$

By subtracting abovementioned equations, solving $\frac{\partial B}{\partial d(i)}$ and substituting it at Eq. (9), we have:

$$\rho(i)+A(i)+pen(i)=\rho_0(i)\left\{1+\frac{d(i)-d_0(i)}{2E(i).d_0(i)}\right\} \quad (11)$$

So, the load profile of the consumers after participation in DRP is as following:

$$d(i)= d_0(i)\left\{1+E(i,i).\frac{[\rho(i)-\rho_0(i)+A(i)+pen(i)]}{\rho_0(i)}\right\} \quad (12)$$

According to (12), if the electricity price does not change and the amount of incentive and penalty neglected, *d(i)* will be the same as $d_0(i)$.

2.1.2. DRP with self and cross elasticity

Based on definition of cross-elasticity which was presented in Eq. (2) and by considering linearization assumptions we have:

$$\frac{\partial d(i)}{\partial \rho(j)}: cons\tan t\ for\ i\ ,j=1,2,...,24 \quad (13)$$

The following linear relationship will be established between price and load:

$$d(i)=d_0(i)+\sum_{\substack{i=1\\ i\neq j}}^{24}E(i,j).\frac{d_0(j)}{\rho_0(j)}.[\rho(i)-\rho_0(i)]\ \ i=1,2,...,24 \quad (14)$$

Now, by taking into account the amount of incentive and penalty, multi-elasticity formulation of DRP will be as following:

$$d(i)=d_0(i).\left\{1+\sum_{\substack{j=1\\ j\neq i}}^{24}E(i,j).\frac{[\rho(i)-\rho_0(i)+A(i)+pen(i)]}{\rho_0(i)}\right\} \quad (15)$$

2.2. Objective formulation

In this part of paper, mathematical formulation for minimization of operation cost and pollution emissions for each hour of next day is presented. Here, f_1 is the cost function in €ct and f_2 is the amount of emissions in kg which must be minimized simultaneously.

$$\begin{aligned} f_1(X(t)) = &\sum_{i=1}^{N_G}[P_{Gi}(t)C_{Gi}(t)+S_{Gi}\left|u_{Gi}(t)-u_{Gi}(t-1)\right|] \\ &+\sum_{i=1}^{Nss}[P_{Si}(t)C_{Si}(t)+S_{Si}\left|u_{Si}(t)-u_{Si}(t-1)\right|] \\ &+P_{EX}(t)C_{EX}(t) \end{aligned} \quad (16)$$

$$\begin{aligned} f_2(X(t)) = &\sum_{i=1}^{N_G}[P_{Gi}(t).E_{Gi}(t)] \\ &+\sum_{j=1}^{Nss}[P_{Sj}(t).E_{Sj}(t)]+P_{EX}(t).E_{EX}(t) \end{aligned} \quad (17)$$

In these equations $P_{Gi}(t)$, $P_{Si}(t)$ and $P_{EX}(t)$ are the hourly power of DGs, storage system and exchanged power with UG, respectively. Furthermore, $C_{Gi}(t)$, $C_{Si}(t)$ and $C_{EX}(t)$ are the suggested price for each hour by DGs, storage system and UG, respectively. u(t) indicates the on/off state of DGs and storage devices. S_{Gi} and S_{Si} are start-up and shut-down costs of DGs and storage device, respectively. However, when the specified unit is off or separated from the microgrid, these costs are zero. Negative value for hourly power of storage system indicates charging or selling power to the UG. Total amount of pollution *E(t)* generated by each unit equals to summation of SO2, CO2 and NOx. Totally, by assuming *X(t)* as the vector of variables which is expressed in Eq. (18), there exists $2(N_G+N_{SS})+1$ variables for each hour of next day that must be calculated using multi-objective optimization method.

$$\begin{aligned} X(t)=[&P_{G1}(t),P_{G2}(t),...,P_{GN_G}(t),P_{S1}(t),P_{S2}(t) \\ &,...,P_{SN_{SS}}(t),P_{Ex}(t),u_{G1}(t),u_{G2}(t),..., \\ &u_{GN_G}(t),u_{S1}(t),u_{S2}(t),...,u_{SN_{SS}}(t)] \end{aligned} \quad (18)$$

2.3. Constraints

The constraints related to multi-objective microgrid EMS problem includes power balance, limitations of generated power of DGs, restrictions related to charge and discharge of storage system as well as constraints related to SOC of storage system. The generation-consumption constraint is formulated as bellow:

$$\sum_{i=1}^{N_G}P_{Gi}(t)+\sum_{j=1}^{N_{SS}}P_{Sj}(t)+P_{EX}(t)=P_{load}(t) \quad (19)$$

In addition, generated power by DGs must be within their limitations:

$$u_{Gi}(t)P_{Gi,\min}\le P_{Gi}(t)\le u_{Gi}(t)P_{Gi,\max}\quad i=1,2,...,N_G \quad (20)$$

The power exchange with UG is restricted as bellow:

$$P_{Ex,\min}\le P_{Ex}(t)\le P_{Ex,\max} \quad (21)$$

Limitations related to storage's rate of charge and discharge for each hour must be established as:

$$u_{Sj}(t)P_{Sj,\min} \le P_{Sj}(t) \le u_{Sj}(t)P_{Sj,\max} \quad j = 1,2,...,N_{SS} \quad (22)$$

Furthermore, SOC constraint of storage system is as bellow:

$$W_{Sj,\min} \le W_{Sj}(t) \le W_{Sj,\max} \quad j = 1,2,...,N_{SS} \quad (23)$$

Here, $W_{Sj}(t)$ is the SOC of j^{th} storage unit which is computed as following at the end of each hour:

$$W_{Sj}(t) = W_{Sj,initial} - \sum_{k=1}^{t} R_{Sj}(k) \quad j = 1,2,...,N_{SS}$$
$$R_{Sj}(k) = \begin{cases} P_{Sj}(k)\eta_{ch\,argej} & if \quad P_{Sj}(k) \le 0 \\ P_{Sj}(k)/\eta_{disch\,argej} & if \quad P_{Sj}(k) > 0 \end{cases} \quad (24)$$

Where, $\eta_{ch\,argej}$ and $\eta_{disch\,argej}$ are the storage's charge and discharge efficiency, respectively.

3. Multi-objective group search optimization algorithm

Multi-objective optimization methods optimize various objective functions simultaneously. This method leads to find various optimized solutions based on dominance concept which are named Pareto fronts. Assume that $f_i(X) = (i = 1,2,....n)$ are the objective functions that must be optimized according to various constraints. Considering X_a and X_b as two feasible solutions, X_a dominates X_b while:

$$\forall k \in \{1,2,...,n\} : f_k(X_a) \le f_k(X_b) \; and$$
$$\exists j \in \{1,2,...,n\} : f_j(X_a) < f_j(X_b) \quad (25)$$

It means that solutions of optimal Pareto will never be dominated by another feasible solution of search space. The optimal Pareto is achieved by drawing optimal solutions of each objective function. In the following, a brief introduction about single-objective GSO algorithm is presented. Then, its multi-objective version is introduced. At last, its stepwise implementation on solving microgrid management problem is expressed.

3.1. Single-objective GSO

GSO [23] is a new optimization algorithm which is based on search behavior of animals and theory of group life among them. GSO population is called a group while each person is called a member. In a n-dimensional search space, the current position and head angle of the i^{th} member in k^{th} iteration is $X_i^K \in R^N$ and $\varphi_i^k = (\varphi_{i_1}^k,...,\varphi_{i_{(n-1)}}^k) \in R^{n-1}$, respectively. The search direction of i^{th} member which is shown by $D_i^k(\varphi_i^k) = (d_{i_1}^k,...,d_{i_{(n-1)}}^k) \in R^{n-1}$ is computed as bellow:

$$d_{i_1}^k = \prod_{q=1}^{n-1} \cos(\varphi_{i_q}^k)$$
$$d_{i_j}^k = \sin(\varphi_{i_{(j-1)}}^k) \prod_{q=j}^{n-1} \cos(\varphi_{i_q}^k) \quad (j = 2,...,n-1) \quad (26)$$
$$d_{i_n}^k = \sin(\varphi_{i_{(n-1)}}^k)$$

GSO population is composed of three kinds of members including producer, scroungers and rangers. Scroungers try hard to reach producer while rangers have random movements. For simplicity, it is assumed that there is only one producer and the rest of population are scroungers (with probability γ) and rangers (with probability 1-γ). In each iteration, the member who has the best objective function is chosen as the producer. The search process of this algorithm is based on animals' vision ability. So, the search space is divided into n dimensions while the maximum head angle and search radians are $\theta_{\max} \in R^1$ and $l_{\max} \in R^1$, respectively. Demonstration of the algorithm in a three-dimensional space is shown in Fig. 1. The maximum pursuit angle is $\pi/a2$ while the constant a is given by round ($\sqrt{N_{variable}+1}$). The maximum pursuit distance is calculated by $\sqrt{\sum_{i=1}^{N_{variable}} (U_i - L_i)}$. More explanation about parameters of GSO algorithm can be found in [24].

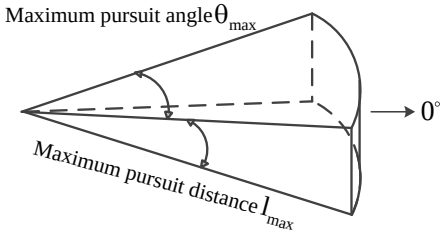

Fig. 1. Three-dimensional search space

The angle corner shows the location of producer whose XP changes during k^{th} iteration by sampling three points in the search space as following:

$$X_z = X_P^k + r_1 l_{\max} D_P^k(\varphi^k) \quad (27)$$

$$X_r = X_P^k + r_1 l_{\max} D_P^k(\varphi^k + r_2 \theta_{\max}/2) \quad (28)$$

$$X_l = X_P^k + r_1 l_{\max} D_P^k(\varphi^k - r_2 \theta_{\max}/2) \quad (29)$$

Where $r_1 \in R^1$ and $r_2 \in R^{n-1}$ are random numbers and $l_{\max}$ is the length of search vector.

After calculating abovementioned locations, the point which has the best objective function is selected and the producer changes its head angle as:

$$\varphi^{k+1} = \varphi^{k} + r_2 \alpha_{\max} \tag{30}$$

However, if a better location was not found for producer after *a* iterations, its head angle become zero as:

$$\varphi^{k+a} = \varphi^{k} \tag{31}$$

As mentioned above, rest of the members are scroungers and rangers. Scroungers move toward producer by random steps as following:

$$X_i^{k+1} = X_i^{k} + \omega_1 r_3 (X_P^{k} - X_i^{K}) \tag{32}$$

Where, r_3 is a random number between 0 and 1 and ω_1 is accelerating coefficient. If a scrounger finds better location in comparison to existed producer, in the next iteration it will be chosen as the producer.

The remaining of the population which is called ranger has random movements and by computing l_i a random distance moves to a new location as bellow:

$$X_i^{k+1} = X_i^{k} + \omega_2 l_i D_i^{k}(\varphi^{k+1}) \tag{33}$$

Where, ω_2 is the accelerating coefficient.

3.2. Multi-objective GSO (MOGSO)

In this paper, MOGSO along with FDM technique is utilized for solving multi-objective microgrid management problem. In multi-objective optimization, multiple objective functions are minimized simultaneously, as bellow:

$$\begin{aligned} &\min(F(X) = [f_1(X), f_2(X)] \\ &X = [x_1, x_2, ..., x_{144}] \end{aligned} \tag{34}$$

Where, $f_1(X), f_2(X)$ are objective functions and X demonstrates vector of variables. The aim of multi-objective optimization is to find the most feasible solution which meets all of constraints. Considering all of objective functions, it is impossible to confirm a solution is better than others since objective functions may be against each other. Stepwise implementation of MGSO in solving microgrid management problem is explained here:

1) Hourly power of DGs, storage system and UG are considered as the decision making variables and initial population is generated based on legal limitations of variables.

2) The value of objective functions correspond to each population member is computed.

3) In this step, non-dominated solutions are determined which are the optimal ones for a function without worsening other functions.

4) Now, population members are divided into multiple fronts. The first front is completely non-dominated while it dominates the second front. Furthermore, a ranking value is assigned to all members of each front. For instance, ranking number for members of first front is 1.

5) In order to determine proximity of a member to its neighbors, crowding distance is calculated. The greater is the distance, the population will be more diverse. This index for j^{th} member of k^{th} front is calculated as:

$$CD(F_k, j) = \begin{cases} \infty & j = 1, n \\ \sum_{i=1}^{n_{obj}} \dfrac{obj_i(j+1) - obj_i(j-1)}{obj_i^{\max} - obj_i^{\min}} & j = 2,3,...,n \end{cases} \tag{35}$$

6) The population is sorted based on their crowding distance. Sorting will be repeated based on members ranking value.

7) Make new producer, scroungers and rangers based on GSO algorithm.

8) Generated population in the previous step is combined with the existing population. Then they will be sorted based on crowding distance and non-dominancy. Finally, the initial population size of sorted population is saved and the rest are omitted.

9) If the maximum number of iteration or convergence condition is reached, the optimization will stop and the best solution is selected based on FDM technique.

3.3. Fuzzy decision making (FDM) technique

After determining the Pareto fronts, the best solution is selected by using FDM. In this method, i^{th} objective function is mapped on a linear membership function as bellow:

$$\mu_i^k = \begin{cases} 1 & f_i \le f_i^{\min} \\ \dfrac{f_i^{\max} - f_i}{f_i^{\max} - f_i^{\min}} & f_i^{\min} \le f_i \le f_i^{\max} \\ 0 & f_i \ge f_i^{\max} \end{cases} \tag{36}$$

Then, normalized membership function μ^k for k^{th} Pareto front solution is determined.

$$\mu^k = \frac{\sum_{i=1}^{N_{obj}} \mu_i^k}{\sum_{k=1}^{N_{sol}} \sum_{i=1}^{N_{obj}} \mu_i^k} \quad (37)$$

Finally, the maximum weakest solution which has the greatest amount of μ^k is selected as the optimum solution. Overall flowchart of the solving microgrid energy management problem by the proposed MOGSO is shown in Fig. 2.

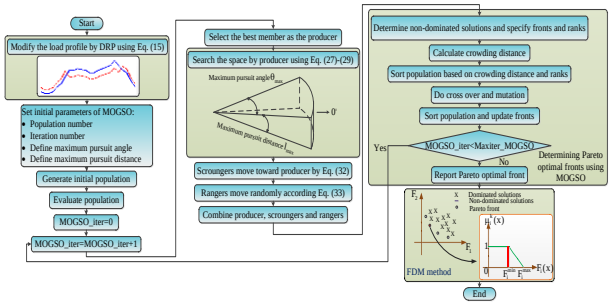

Fig. 2. Flowchart of solving microgrid management using MOGSO

4. Results and discussions

In this section, numerical studies are presented. First of all understudying microgrid is introduced. Then, simulation and analytical results are presented in various scenarios. The experiments are performed using MATLAB R2013a, running on a laptop with a 1.5 GHz AMD Quad core A4 CPU and 4GB RAM memory, and Microsoft Windows 8.1.

4.1. Parameter selection

The maximum number of iterations is set to 100 and the population size of 100 is used for all of scenarios. In addition, the maximum pursuit angle and maximum pursuit distance are considered to be 0.0218 and 455.27, respectively. To determine the parameters of the utilized GSO algorithm, a number of simulations is done using benchmark function $f(x) = \sum_{i=1}^{n-1}\left[100(x_{i+1} - x_i^2)^2 + (x_i - 1)^2\right]$. Table 1 presents the mean value of function over 50 trial runs. According to this table ω_1=2, ω_2=3 and γ=0.95 leads to better solution.

Table 1. Effects of the GSO parameters on optimization of f

ω_1	ω_2	γ	Mean	ω_1	ω_2	γ	Mean
1	1	0.75	544.18	2	2	0.95	71.27
1	1	0.85	122.77	2	3	0.75	1223.2
1	1	0.95	50.01	2	3	0.85	93.53
1	2	0.75	4703.9	**2**	**3**	**0.95**	**32.28**
1	2	0.85	158.47	3	1	0.75	2769.5
1	2	0.95	69.46	3	1	0.85	105.8
1	3	0.75	3318.7	3	1	0.95	64.7
1	3	0.85	522.73	3	2	0.75	5481.4
1	3	0.95	66.94	3	2	0.85	118.1
2	1	0.75	1151.2	3	2	0.95	92.3
2	1	0.85	60.62	3	3	0.75	1269.3
2	1	0.95	35.59	3	3	0.85	154.01
2	2	0.75	2659.3	3	3	0.95	96.41
2	2	0.85	107.01				

4.2. Case study

The understudying test system is a microgrid that is composed of a MT, FC, PV and WT as DGs as well as a battery as the energy storage system while its single-line diagram is shown in Fig. 3.

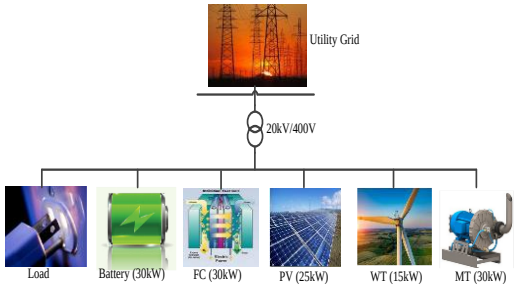

Fig. 3. The understudying microgrid [3]

It is assumed that the microgrid is connected to the UG. The hourly forecasted values for load and power market price are shown in Fig. 4. The hourly generated power by WT and PV are given in Table 2. The charge and discharge efficiency of the battery is assumed to be 0.9.

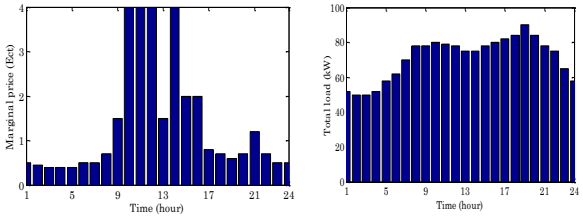

(a) (b)

Fig. 4. The hourly values of (a) market price (b) Load [3]

Table 2. Hourly forecasted values for WT and PV power generation [3]

Hour	WT	PV	Hour	WT	PV
1	5.25	0	13	10.5	23.75
2	5.25	0	14	6.3	22.5
3	5.25	0	15	5.25	7.5

4	5.25	0	16	4.2	4.5
5	5.25	0	17	5.25	2.5
6	3.5	0	18	5.25	0
7	5.25	0	19	4.2	0
8	4.2	0	20	5.25	0
9	5.25	4	21	4.2	0
10	7	7.5	22	4.2	0
11	21	10	23	3.85	0
12	24.5	12.5	24	3.5	0

The limits related to generated and exchanged power, bidding and pollution price of DGs, storage system and UG are given in Table 3.

Table 3. Limits of generated and exchanged power, bidding and pollution price of DGs, storage system and UG [3]

DG type	Min. power (kW)	Max. power (kW)	Bid (€ct/kWh)	Start-up/ shut-down	CO_2 (kg/MWh)	SO_2 (kg/MWh)	NO_x (kg/MWh)
MT	6	30	0.457	0.96	720	0.0036	0.1
FC	3	30	0.294	1.65	460	0.003	0.0075
PV	0	25	2.584	0	0	0	0
WT	0	15	1.073	0	0	0	0
Battery	-30	30	0/380	0	10	0.0002	0.001
UG	-30	30	Fig. 4 (a)	0	0	0	0

In this paper, load curve is divided into three periods including low-load period (1:00 am-7:00 am), off-peak period (8:00 am-20:00 pm) and peak period (20:00 pm-0:00 am). The elasticity coefficients corresponding to each period are given in Table 4 [25].

Table 4. Self and cross elasticity coefficients [25]

	Low-load	Off-peak	Peak
Low-load	-0.1	0.016	0.012
Off-peak	0.016	-0.1	0.01
Peak	0.012	0.01	-0.1

4.3. Simulation results

Simulation results related to microgrid EMS are analyzed in three scenarios as bellow:

1) Single-objective minimization of cost
2) Single-objective minimization of emission
3) Multi-objective minimization of cost and emission

All of the abovementioned scenarios are studied in two modes, with and without considering DRP. The modification in load curve in response to DRP is shown in Fig. 5. It can be seen that load consumption is transferred from peak and expensive hours to the low-load and cheap durations. In the following, the dashed curve of the Fig. 5 is considered as the load curve in the presence of DR program.

4.3.1. Scenario 1: Single-objective minimization of cost

In this section, the power generation cost of microgrid is minimized in two cases: absence and in the presence of DRP. During these two cases, DGs, battery and UG are ON and programmable.

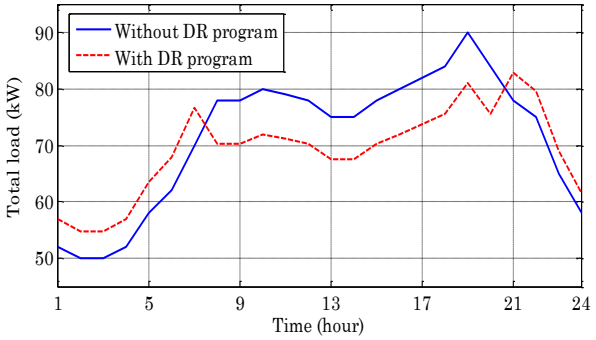

Fig. 5. Load curve with and without considering DR program

The DRP is neglected in the first case. However, the latter case has considered DRP. The convergence process of GSO algorithm in solving two cases of this scenario are shown in Fig. 6.

The hourly simulation results for the first and second case are expressed in Table 5 and 6, respectively.

Table 5. Scenario 1: The optimal solution without considering DR (Total cost=737.23)

Hour	MT (kW)	FC (kW)	PV (kW)	WT (kW)	Battery (kW)	UG (kW)
1	7.79	30	0	1.32	-6.24	19.12
2	29.85	3.98	0	3.58	28.45	-15.86
3	16.04	30	0	1.45	-25.11	27.61
4	7.9	30	0	2.55	-3.79	15.33
5	26.62	30	0	0.28	-13.11	14.19
6	20.7	30	0	3.31	23.78	-15.89
7	13.06	30	0	2.22	-5.28	30
8	19.97	30	0	2.52	-3.37	28.87
9	17.23	30	0.48	0.17	7.58	22.52
10	15.33	30	3.6	0.96	22.75	7.34
11	6.53	30	1.41	0.55	17.08	23.41
12	27.72	30	3.33	19.11	25.91	-28.09

13	9.8	30	9.64	4.67	27.14	-6.28
14	24.89	30	17.1	3.78	27.14	-27.93
15	28.85	30	2.94	3.35	16.58	-3.74
16	26.48	30	2.59	0.54	24.58	-4.21
17	7.94	30	2.5	1.2	10.35	30
18	24.71	30	0	5.19	13.18	10.9
19	8.38	30	0	1.41	20.19	30
20	24.33	30	0	0.31	12.5	16.84
21	10.98	30	0	2.17	29.5	5.33
22	16.67	30	0	1.92	-3.6	30
23	26.65	30	0	2.11	23.68	-17.45
24	11.82	30	0	2.74	-16.56	30

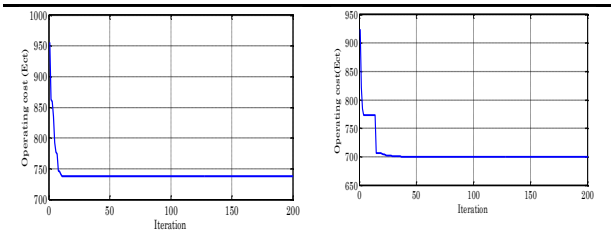

(a) (b)

Fig. 6. Scenario 1: Convergence process of GSO in minimizing cost a) without DR b) with DR

According to Table 5, during the first hours of the day in which electricity is cheaper, the battery is charged. However, in peak hours which are expensive, the UG buys power from the microgrid to supply its own demand. As a result of low cost of electricity produced by FC, this DG works at its maximum capacity during most hours of the day to minimize the cost. In the following, participation of consumers in DR has modified the load curve and according to Table 6 generated power by PV and WT are reduced. It is clear that WT has generated more power in comparison to PV since being cheaper. In addition to peak shaving, DR has caused to reduce the cost by 5%.

Table 6. Scenario 1: The optimal solution with considering DR (Total cost=699.86)

Hour	MT (kW)	FC (kW)	PV (kW)	WT (kW)	Battery (kW)	UG (kW)
1	10.58	30	0	0.84	12.76	2.77
2	14.88	28.82	0	1.73	-7.59	16.93
3	9.89	30	0	3.84	-18.95	29.99
4	29.64	27.42	0	1.25	24.16	-25.51
5	12.07	30	0	2.19	2.91	16.35
6	29.1	30	0	0.57	-0.76	9.01
7	12.65	30	0	3.24	12.37	18.42
8	16.59	30	0	2.6	21.71	-0.71
9	17.69	30	2.37	0.17	12.49	7.46
10	18.96	30	3.32	1.57	10.66	7.47
11	14.13	30	2.99	19.28	23.88	-19.19
12	11.54	30	3.9	21.83	23.1	-25.19
13	12.95	30	21.17	0.009	22.64	-19.27
14	19.91	30	12.88	4.51	8.12	-4.92
15	22.85	30	0.92	1.61	29.3	-14.5
16	9.47	30	4.5	1.06	-2.98	29.94
17	12.2	30	2.07	1.93	9.79	17.78
18	13.23	30	0	1.55	3.38	27.42
19	20.63	30	0	2.33	-1.82	29.85
20	26.36	30	0	2.54	9.47	7.21
21	25.42	30	0	2.67	-3.67	28.36
22	16.21	30	0	1.54	9.69	22.14
23	21.69	30	0	2.82	-15.02	22.49
24	24.04	30	0	0.5	27.27	-20.25

4.3.2. Scenario 2: Single-objective minimization of emission

In this scenario, GSO is utilized to minimize the emission in two cases. During the first case, DR is neglected while it is considered in the second case. Convergence process of GSO for these two cases are shown in Fig. 7.

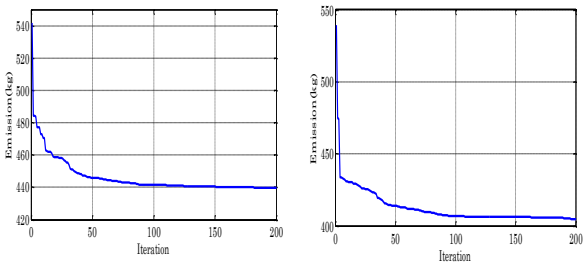

(a) (b)

Fig. 7 Scenario 2: Convergence process of GSO in minimizing emission a) without DR b) with DR

Hourly simulation results for both cases are expressed in Tables 7 and 8, respectively. Since WT and PV are free of emission, their hourly power are the same as previous scenario and have not changed significantly.

Table 7. Scenario 2: The optimal solution without considering DR (Total emission=439.69)

Hour	MT (kW)	FC (kW)	PV (kW)	WT (kW)	Battery (kW)	UG (kW)
1	13.36	3	0	1.5	25.46	8.66
2	16.99	20.77	0	3.44	9.31	-0.52
3	9.68	17.06	0	0.99	16.66	5.58
4	13.2	10.12	0	0.78	7.6	20.27
5	18.76	13.19	0	4.87	-8.82	30
6	9.86	3	0	2.1	18.57	28.44
7	18.84	3	0	0	29.85	18.3
8	15.24	13.9	0	1.16	17.68	30
9	20.15	16.4	0.54	3.83	7.05	30
10	17.97	3	1.85	2.59	27.29	27.28
11	10.2	29.95	10	5.35	-6.51	30

12	7.25	13.19	0.73	1.16	25.64	30
13	12.44	25.23	3.26	3.5	0.55	30
14	26.48	17.91	4.51	6.1	-10.01	30
15	25.35	3	1.6	4.84	18.62	24.56
16	10.73	11.04	1.19	3.19	23.83	30
17	14.17	29.64	2.5	4.89	0.78	30
18	13.88	12.12	0	1.79	26.19	30
19	24.01	29.27	0	3.52	3.18	30
20	11.27	28.98	0	1.08	2.65	30
21	15.98	3	0	3.86	28.55	26.58
22	28.2	3	0	2.51	25.03	16.25
23	20.08	6.44	0	1.66	6.79	30
24	16.35	21.76	0	1.41	-11.53	30

Table 8. Scenario 2: The optimal solution with considering DR (Total emission=404.45)

Hour	MT (kW)	FC (kW)	PV (kW)	WT (kW)	Battery (kW)	UG (kW)
1	10.8	7.9	0	5.04	3.21	30
2	8.22	3	0	0.63	15.35	27.56
3	11.2	19.59	0	0.21	-6.23	30
4	22.47	3	0	4.11	0.24	27.63
5	9.5	10.12	0	4.95	8.95	30
6	9.39	29.97	0	1.98	-3.43	30
7	19.5	3	0	1.92	23.41	28.84
8	7.37	10.01	0	0.69	22.11	30
9	17.49	3	1.49	1.14	24.18	22.88
10	29.62	3	1.46	3.39	23.93	10.01
11	29.26	3	7.8	0.34	10.13	20.55
12	16.66	3	4.67	16.69	13.67	15.48
13	21.07	3	12.42	10.45	-3.11	23.65
14	18.49	21.04	5.29	2.81	-10.15	30
15	6.17	3	7.24	0.53	26.95	26.28
16	16.27	25.72	2.8	3.89	-6.7	30
17	9.92	5.48	2.15	3.39	22.83	30
18	19.04	3	0	4.26	28.4	20.88
19	27.18	28.08	0	2.05	-6.32	30
20	13.75	27.08	0	3.19	1.57	30
21	7.47	24.33	0	1.91	19.06	30
22	20.48	24.7	0	3.84	0.57	30
23	12.21	3	0	0.18	30	23.58
24	21.93	3	0	2.09	19.91	17.61

In addition, UG does not have emission, too. So, in this scenario microgrid buys power from UG to minimize the existed emission. Based on simulation results of this scenario, considering DR has a sufficient effect on reducing emission and reduced it by 8%.

4.3.3. Scenario 3: Multi-objective minimization of cost and emission

Simultaneous minimization of cost and emission as a multi-objective problem is solved using MOGSO in this scenario. Like two previous scenarios, this scenario is solved in two cases, too. The first one manages microgrid without DR while the second considers the effect of DR. The Pareto fronts proportional to the first and second case are shown in Figs. 8 and 9, respectively. The best solution of each case is marked by a red star which is selected by FDM technique. The cost and emission conflict each other. It means that moving from one end of Pareto front to the other end maximizes cost and minimizes emission and vice versa. So, FDM technique have been employed to choose the best solution.

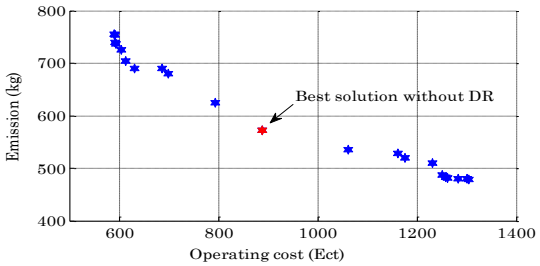

Fig. 8. Scenario 3: Pareto front of MOGSO without DR

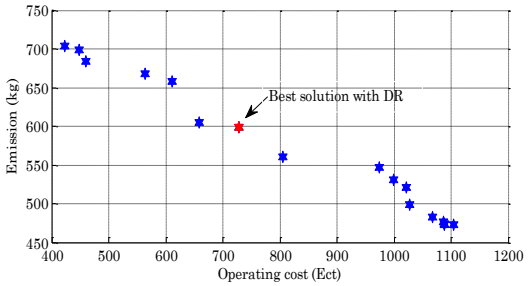

Fig. 9. Scenario 3: Pareto front of MOGSO with DR

Table 9 and 10 show the values of both objective functions Pareto optimal solutions without and with DR, respectively. Among these optimal solutions, the maximum weakest solution is chosen as the best one.

Table 9. Scenario 3: Pareto optimal solutions without DR

Solution #(k)	f_1 (Ect)	f_2 (kg)	$\frac{(f_1^{max}-f_k)}{(f_1^{max}-f_1^{min})}$	$\frac{(f_2^{max}-f_k)}{(f_2^{max}-f_2^{min})}$	Min
1	1304.3	478.88	0	1	0
2	589.76	754.84	1	0	0
3	**888.93**	**571.91**	**0.5813**	**0.6629**	**0.5813**
4	794.53	625.2	0.7134	0.4698	0.4698
5	1061.3	535.27	0.3401	0.7957	0.3401
6	699.07	679.7	0.847	0.2723	0.2723
7	1230.7	509.82	0.1029	0.8879	0.1029

8	1161.2	528.87	0.2002	0.8189	0.2002
9	1175.1	520.23	0.1808	0.8502	0.1808
10	613.26	704.81	0.9671	0.1813	0.1813
11	630.92	690.12	0.9424	0.2345	0.2345
12	604.78	725.56	0.9790	0.1061	0.1061
13	1250.7	487.75	0.075	0.9679	0.075
14	687.03	689.45	0.8639	0.2370	0.2370
15	594.06	737.45	0.994	0.0630	0.0630
16	591.8	740.11	0.9971	0.0534	0.0534
17	1283.7	480.47	0.0287	0.9943	0.0287
18	591.27	753.47	0.9979	0.005	0.005
19	1260.8	481.1	0.0609	0.9920	0.0609
20	1257.2	482.85	0.0659	0.9856	0.0659
21	1301.01	480.29	0.0046	0.9949	0.0046

Table 10. Scenario 3: Pareto optimal solutions with DR

Solution #(k)	f_1 (Ect)	f_2 (kg)	$\frac{(f_1^{max}-f_k)}{(f_1^{max}-f_1^{min})}$	$\frac{(f_2^{max}-f_k)}{(f_2^{max}-f_2^{min})}$	Min
1	422.85	704.3	1	0	0
2	1103.7	472.71	0	1	0
3	805.29	561.07	0.4383	0.6185	0.4383
4	658.6	604.64	0.6537	0.4303	0.4303
5	974.55	547.41	0.1897	0.6774	0.1897
6	611.37	658.6	0.7231	0.1973	0.1973
7	**728.19**	**598.58**	**0.5515**	**0.4565**	**0.4565**
8	563.66	667.31	0.7932	0.1597	0.1597
9	459.32	683.6	0.9464	0.0894	0.0894
10	1027.6	499.05	0.1118	0.8862	0.1118
11	1067.4	483.22	0.0533	0.9546	0.0533
12	999.86	530.33	0.1525	0.7512	0.1525
13	1020.9	520.95	0.1217	0.7917	0.1217
14	448.44	698.44	0.9624	0.0253	0.0253
15	1087.1	476.09	0.0244	0.9854	0.0244
16	1088.6	472.71	0.0223	1	0.0223
17	1088.5	473.84	0.0223	0.9951	0.0223

Table 11. Scenario 3: The optimal solution without considering DR (Total cost=888.93, Total emission=571.91)

Hour	MT (kW)	FC (kW)	PV (kW)	WT (kW)	Battery (kW)	UG (kW)
1	27.36	4.06	0	3.76	13.36	3.44
2	26.33	4.51	0	3.98	13.44	1.71
3	26.88	5.16	0	3.96	14.61	-0.62
4	25.01	6.09	0	4.26	16.87	-0.24
5	27.09	7.41	0	3.94	13.49	6.04
6	26.39	9.29	0	2.5	12.66	11.14
7	24.83	11.98	0	4.37	14.19	14.61
8	27.33	16.71	0	3.39	13.37	17.18
9	27.08	21.28	3.5	4.73	18.17	4.21
10	27.03	27.01	6.61	5.82	17.59	-4.08
11	24.38	25.77	7.48	17.54	13.04	-9.23
12	24.1	24.02	8.76	20.68	21.54	-21.12
13	25.77	27.54	20.41	7.83	14.1	-14.67
14	26.61	18.04	18.43	4.93	20.82	-13.85
15	23.62	13.08	5.89	4.51	19.04	11.83
16	25.54	6.07	3.86	3.02	15.73	25.75
17	26.35	5.24	1.86	4.3	14.23	30
18	24.67	9.58	0	9.79	15.93	30
19	25.21	9.77	0	3.62	21.38	30
20	25.93	3	0	4.08	21.6	29.37
21	24.99	6.2	0	2.94	13.85	30
22	24.23	3	0	2.98	19.51	25.25
23	26.81	3	0	2.9	16.08	16.18
24	25.84	3	0	2.96	19.41	6.77

Table 12. Scenario 3: The optimal solution with considering DR (Total cost=728.19, Total emission=598.58)

Hour	MT (kW)	FC (kW)	PV (kW)	WT (kW)	Battery (kW)	UG (kW)
1	25.82	9.82	0	4.6	23.4	-6.68
2	26.05	12.71	0	3.69	15.37	-3.06
3	23.8	16.84	0	4.69	12.38	-2.95
4	26.18	22.71	0	4.04	14.34	-10.31
5	24.84	26.97	0	4.11	12.09	-4.48
6	27.1	25.7	0	2.7	22.4	-9.99
7	22.97	24.08	0	3.94	20.22	5.46
8	22.89	28.88	0	3.45	20.14	-5.17
9	26.85	28.41	3.15	4.02	15.75	-8
10	23.95	27.74	6.02	6.28	23.58	-15.6
11	25.03	25.08	7.86	18.26	21.62	-26.78
12	25.56	14.73	10.86	21.37	23.07	-25.41
13	26.44	23.46	18.39	8.32	14.07	-23.2
14	25.56	20.68	19.27	5.02	12.47	-15.25
15	24.32	16.73	5.72	4.11	14.04	5.25
16	27.42	11.09	3.47	3.59	18	8.4
17	22.99	3.06	2	3.97	19.71	22.04
18	22.82	3	0	3.88	17	28.88
19	22.81	3.29	0	3.09	21.79	30
20	26.06	3	0	3.77	15.98	26.78
21	27.06	5.02	0	3.62	17.07	30
22	25.22	5.14	0	3.12	16.11	30
23	25.28	3	0	3.24	18.12	19.33
24	23.85	3	0	2.67	23.54	8.48

Hourly simulation results of this scenario without and with considering effects of DRP are expressed in Tables11 and 12, respectively. Based on these results, DR has reduced the cost and emission by 26% and 19%, respectively.

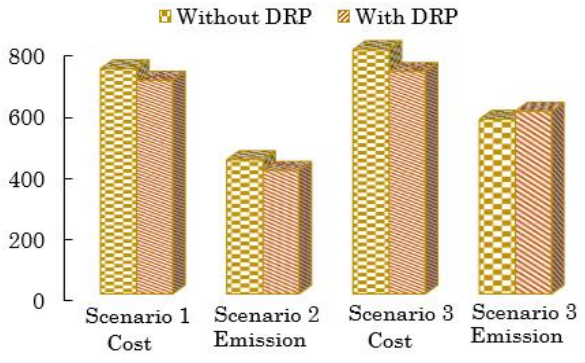

Fig. 10. Comparing results of all scenarios

A comparision between results of all scenarios is depicted in Fig. 10. It can be seen that during the first and second scenarions, single objective optimization has reached to optimum value of cost and emission. However, during the third scenarion, although the cost and emission functions conflict each other, MOGSO has resulted in the optimum cost and emission simoultanously. According to Fig. 10 MOGSO is more successful in reducing total cost.

Conclusions

Recently, DGs are utilized near consumers to supply their demand within a microgrid. However, the generated power by DGs and load has stochastic nature and are uncertain. As a result, this paper tried to tackle this problem by using flexible power sources such as DRP and battery. The microgrid EMS problem has been solved with the aim of minimizing the total cost and emission in the presence and absence of DRP. For better analysis, simulations have been implemented in three different scenarios while considering microgrid management as a single-objective and multi-objective problem. GSO algorithm has been utilized to solve single-objective problems while MOGSO along with FDM technique are employed to simultaneous minimization of cost and emission. Simulation results approve that GSO and MOGSO are successful in decreasing the total cost and emission. Reducing the cost results in charging the battery during cheap hours to discharge it in expensive periods. To reach lower cost value, the cheapest DG, here FC, works at its maximum capacity and the generation power by WT is more than PV as a result of being cheaper. When minimizing emission, the microgrid buys power from UG since it is free of emission. Utilizing DRP as a flexible energy source not only covers uncertainties of wind and solar power but also minimizes cost and emission by reducing utilization of expensive DGs. Totally, solving the microgrid EMS problem using the proposed MOGSO has caused more reduction in operation cost in comparison to the emission.

References

[1] C. Yin, H. Wu, F. Locment, and M. Sechilariu, "Energy management of DC microgrid based on photovoltaic combined with diesel generator and supercapacitor," *Energy Convers. Manage.*, vol. 132, pp. 14-27, 2017.

[2] E. Hossain, E. Kabalci, R. Bayindir, and R. Perez, "Microgrid testbeds around the world: State of art," *Energy Convers. Manage.*, vol. 86, pp. 132-153, 2014.

[3] A. Deihimi, B. Keshavarz Zahed, and R. Iravani, "An interactive operation management of a micro-grid with multiple distributed generations using multi-objective uniform water cycle algorithm," *Energy*, vol. 106, pp. 482-509, 2016.

[4] E. E. Sfikas, Y. A. Katsigiannis, and P. S. Georgilakis, "Simultaneous capacity optimization of distributed generation and storage in medium voltage microgrids," *Int. J. Electr. Power Energy Syst.*, vol. 67, pp. 101-113, 2015.

[5] M. Marzband, F. Azarinejadian, M. Savaghebi, and J. M. Guerrero, "An optimal energy management system for islanded microgrids based on multiperiod artificial bee colony combined with markov chain," *IEEE Syst. J.*, vol. PP, pp. 1-11, 2015.

[6] T. Wu, Q. Yang, Z. Bao, and W. Yan, "Coordinated energy dispatching in microgrid with wind power generation and plug-in electric vehicles," *IEEE Trans. Smart Grid*, vol. 4, pp. 1453-1463, 2013.

[7] J. Garcia-Gonzalez, R. M. R. d. l. Muela, L. M. Santos, and A. M. Gonzalez, "stochastic joint optimization of wind generation and pumped-storage units in an electricity market," *IEEE Trans. Power Syst.*, vol. 23, pp. 460-468, 2008.

[8] L. Guo, W. Liu, X. Li, Y. Liu, B. Jiao, W. Wang, "Energy management system for stand-alone wind-powered-desalination microgrid," *IEEE Trans. Smart Grid*, vol. 7, pp. 1079-1087, 2016.

[9] M. Motevasel and A. R. Seifi, "Expert energy management of a micro-grid considering wind energy uncertainty," *Energy Convers. Manage.*, vol. 83, pp. 58-72, 2014.

[10] C.S. Karavas, G. Kyriakarakos, K. G. Arvanitis, and G. Papadakis, "A multi-agent decentralized energy management system based on distributed intelligence for the design and control of autonomous poly generation microgrids," *Energy Convers. Manage.*, vol. 103, pp. 166-179, 2015.

[11] S. A. Alavi, A. Ahmadian, and M. Aliakbar-Golkar, "Optimal probabilistic energy management in a typical micro-grid based-on robust optimization and point estimate method," *Energy Convers. Manage.*, vol. 95, pp. 314-325, 2015.

[12] M. A. Fotouhi Ghazvini, J. Soares, N. Horta, R. Neves, R. Castro, and Z. Vale, "A multi-objective model for scheduling of short-term incentive-based demand response programs offered by electricity retailers," *Appl. Energy*, vol. 151, pp. 102-118, 2015.

[13] H. A. Aalami, M. P. Moghaddam, and G. R. Yousefi, "Demand response modeling considering Interruptible/ Curtailable loads and capacity market programs," *Appl. Energy*, vol. 87, pp. 243-250, 2010.

[14] L. Wang, Q. Li, R. Ding, M. Sun, and G. Wang, "Integrated scheduling of energy supply and demand in

microgrids under uncertainty: A robust multi-objective optimization approach," *Energy*, vol. 130, pp. 1-14, 2017.
[15] M. Mazidi, A. Zakariazadeh, S. Jadid, and P. Siano, "Integrated scheduling of renewable generation and demand response programs in a microgrid," *Energy Convers. Manage.*, vol. 86, pp. 1118-1127, 2014.
[16] G. R. Aghajani, H. A. Shayanfar, and H. Shayeghi, "Presenting a multi-objective generation scheduling model for pricing demand response rate in micro-grid energy management," *Energy Convers. Manage.*, vol. 106, pp. 308-321, 2015.
[17] R. Wang, P. Wang, G. Xiao, and S. Gong, "Power demand and supply management in microgrids with uncertainties of renewable energies," *Int. J. Electr. Power Energy Syst.*, vol. 63, pp. 260-269, 2014.
[18] H. Safamehr and A. Rahimi-Kian, "A cost-efficient and reliable energy management of a micro-grid using intelligent demand-response program," *Energy*, vol. 91, pp. 283-293, 2015.
[19] Y. Simmhan, S. Aman, A. Kumbhare, R. Liu, S. Stevens, Q. Zhou, "Cloud-based software platform for big data analytics in smart grids," *Comput. Sci. Eng.*, vol. 15, pp. 38-47, 2013.
[20] W. Alharbi and K. Raahemifar, "Probabilistic coordination of microgrid energy resources operation considering uncertainties," *Electr. Power Syst. Res.*, vol. 128, pp. 1-10, 2015.
[21] M. Marzband, M. Ghadimi, A. Sumper, and J. L. Domínguez-García, "Experimental validation of a real-time energy management system using multi-period gravitational search algorithm for microgrids in islanded mode," *Appl. Energy*, vol. 128, pp. 164-174, 2014.
[22] B. Zhao, M. Xue, X. Zhang, C. Wang, and J. Zhao, "An MAS based energy management system for a stand-alone microgrid at high altitude," *Appl. Energy*, vol. 143, pp. 251-261, 2015.
[23] S. He, Q. H. Wu, and J. R. Saunders, "Group search optimizer: an optimization algorithm inspired by animal searching behavior," *IEEE Trans. Evol. Comput.*, vol. 13, pp. 973-990, 2009.
[24] M. Moradi-Dalvand, B. Mohammadi-Ivatloo, A. Najafi, and A. Rabiee, "Continuous quick group search optimizer for solving non-convex economic dispatch problems," *Electr. Power Syst. Res.*, vol. 93, pp. 93-105, 2012.
[25] H. A. Aalami, M. P. Moghaddam, and G. R. Yousefi, "Modeling and prioritizing demand response programs in power markets," *Electr. Power Syst. Res.*, vol. 80, pp. 426-435, 2010.